Biofilm 8 (2024) 100230

Contents lists available at ScienceDirect

Biofilm

journal homepage: www.sciencedirect.com/journal/biofilm

Plasma activated water pre-treatment substantially enhances phage activity against *Proteus mirabilis* biofilms

Akash Shambharkar [a], Thomas P. Thompson [a,1], Laura A. McClenaghan [a,1], Paula Bourke [b], Brendan F. Gilmore [a], Timofey Skvortsov [a,*]

[a] School of Pharmacy, Queen's University Belfast, Medical Biology Centre, 97 Lisburn Road, Belfast, BT9 7BL, UK
[b] Plasma Research Group, School of Biosystems and Food Engineering, University College Dublin, Dublin 4, Ireland

ARTICLE INFO

Keywords:
Bacteriophage
Phage
Cold plasma
Plasma activated water
Proteus mirabilis
Biofilms
Urinary tract infections

ABSTRACT

The ongoing antimicrobial resistance crisis has incentivised research into alternative antibacterial and anti-biofilm agents. One of them is plasma-activated water (PAW), which is produced by exposing water to a cold plasma discharge. This process generates a diverse array of reactive oxygen and nitrogen species (ROS/RNS) with antimicrobial properties. Another intensively studied class of alternative antimicrobials are bacteriophages, attracting attention due to their specificity and strong antibacterial activity. As combinations of different types of antimicrobials are known to often exhibit synergistic interactions, in this study we investigated the combined use of cold atmospheric-pressure plasma-activated water and the bacteriophage vB_PmiS_PM-CJR against *Proteus mirabilis* biofilms as a potential option for treatment of catheter-associated urinary tract infections (CAUTIs).

We compared the effect of two cold plasma discharge setups for PAW production on its antimicrobial efficacy against *P. mirabilis* planktonic and biofilm cultures. Next, we assessed the stability of the phage vB_PmiS_PM-CJR in PAW. Finally, we tested the antimicrobial activity of the phages and PAW against biofilms, both individually and in combinations.

Our findings demonstrate that the combination of PAW with phage is more effective against biofilms compared to individual treatments, being able to reduce the number of biofilm-embedded cells by approximately 4 log. We were also able to show that the order of treatment plays an important role in the anti-biofilm activity of the phage-PAW combination, as the exposure of the biofilm to PAW prior to phage administration results in a stronger effect than the reverse order.

This research underlines PAW's ability to potentiate phage activity, showcasing a considerable reduction in biofilm viability and biomass. Additionally, it contributes to the growing body of evidence supporting the use of phage-based combinatorial treatments. Overall, this sequential treatment strategy demonstrates the potential of leveraging multiple approaches to address the mounting challenge of antibiotic resistance and offers a promising avenue for enhancing the efficacy of CAUTI management.

1. Introduction

Healthcare-associated infections are estimated to cost the UK National Healthcare System (NHS) approximately £2.7 billion a year [1]. Urinary tract infections (UTIs) are among the most common types of healthcare-associated infections, accounting for 17.2 % of all cases in England [2], and up to 80 % of these are catheter-associated urinary tract infections (CAUTI) [3], with a recent study estimating that 12 % of patients who have a catheter inserted for 30 days will develop a CAUTI [4].

Following catheterisation, the presence of *Proteus mirabilis* on the catheter and drainage bag surfaces can be especially dangerous. Production of ureases by *P. mirabilis* is responsible for decomposition of urea in the urine, which increases urinary pH, leading to precipitation of struvite and apatite crystals from the urine and resulting in encrustation and obstruction of urinary catheters [5,6]. Catheter blockage from crystalline biofilms occurs in up to 50 % of patients with long-term (>28 days) catheterisation [7], which necessitates catheter replacement,

* Corresponding author.
E-mail address: t.skvortsov@qub.ac.uk (T. Skvortsov).
[1] these authors contributed equally to this work.

https://doi.org/10.1016/j.bioflm.2024.100230
Received 16 August 2024; Received in revised form 15 October 2024; Accepted 16 October 2024
Available online 18 October 2024

causing patient discomfort, increased risk of urethral tract tissue damage, and higher treatment costs. The crystalline deposits produced by *P. mirabilis* confer additional mechanical and chemical protection (including from antibacterial agents), reduce the anti-attachment efficiency of antimicrobial coatings, and themselves act as attachment points, enabling sequential co-colonisation by other microorganisms. Many key pathogens, including *Proteus* species, are becoming increasingly resistant to antibiotics, with UTIs identified as the fourth leading cause of deaths attributable to antimicrobial resistance (AMR) [8]. Together with the rising challenges posed by biofilm-associated infections, there is a pressing need for innovative antimicrobial approaches.

The use of non-thermal, or 'cold' atmospheric-pressure plasma presents a promising alternative in combatting bacterial pathogens [9]. As a partially ionised gas, cold plasma inactivates bacteria through combined physical and chemical effects resulting from the plasma plume. This plume produces a complex mixture of reactive oxygen species (ROS) and reactive nitrogen species (RNS), which compromise bacterial cell membrane and damage DNA, displaying broad-spectrum antimicrobial effects, including against the ESKAPE pathogens [10]. Recent work has focused on the generation of plasma activated water (PAW) and other liquids from cold plasma exposure. PAW, instilled with many of the reactive species present in the cold plasma, exhibits bactericidal activity against both planktonic and biofilm phenotypes similarly to cold plasma. This circumvents the need for a close and direct contact between the plasma discharge and the target surface. Cold plasma and PAW have been used in combinations with other antimicrobial agents, enchaining the efficacy of treatments. For instance, the role of sub-lethal plasma treatment was shown to enhance the susceptibility of *Pseudomonas aeruginosa* biofilms to conventional antibiotics [11].

Another emerging approach is bacteriophage (phage) therapy, which exhibits remarkable specificity, unlike broad-spectrum antibiotics, minimising collateral damage to the beneficial non-target microbiota [12]. Phages are also effective against antibiotic-resistant strains [13]. The fundamental differences between phages compared to other antibacterial agents can enhance combinatorial treatments, resulting in synergistic antibacterial effects. While most research has investigated phage-antibiotic combinations [14,15], there is growing interest in integrating phages with other novel approaches including cold plasma. For example, Cui et al. combined a cold nitrogen plasma with phages to eradicate *Escherichia coli* O157:H7 biofilms on vegetables [16], and Gu et al., 2022 observed that plasma treatment triggered prophage activation in *E. coli* biofilms, leading to biofilm disruption [17].

Building upon these innovative approaches, our study investigates the synergistic effects of bacteriophages and PAW in targeting the biofilms of *P. mirabilis*. The study encompasses two objectives: the first is to explore how the variations in plasma discharge parameters, such as design and power, influence the antimicrobial efficacy of PAW. The cold plasma generator system used in this study has a relatively simple design utilizing atmospheric air as a source of ionisable gas, thus offering a cost-effective solution to make PAW. Depending upon the position of ground electrode and voltage settings, two distinct modes of operation could be used, Spark and Glow, which are characterised by the behaviour of the plasma plume generation. Spark plasma is produced in discrete discharges while Glow has a continuous discharge. The differences in the operational conditions result in the production of specific reactive species and manifest in distinct properties of the water samples exposed to different plasma discharge types. The reactive species generated as well as the chemical and physical properties of the liquid exposed to both plasma sources are known to differ substantially [18,19].

The second objective is to determine the interactive dynamics between bacteriophages and PAW when applied to biofilms — whether these interactions are synergistic, enhancing the biofilm eradication, or antagonistic, detracting from their individual effectiveness. By conducting this dual-focused inquiry, we aim to shed light on the potential of leveraging bacteriophages and PAW in concert to overcome the formidable defence mechanisms of *P. mirabilis* biofilms, thereby contributing to the development of more effective strategies for infection control and antimicrobial resistance mitigation.

2. Materials and methods

2.1. Bacteria and phage used in this study

The bacterial strain *Proteus mirabilis* BB2000 [20] was maintained on lysogeny broth (LBB) (Invitrogen, Paisley, UK). The phage, vB_PmiS_PM-CJR, previously isolated and characterised by our group [21], was propagated in a liquid culture of *P. mirabilis*. The concentrated phage stock was then stored at 4 °C. Both the phage titre determination using a spot test and the double-layer plaque assay method are previously described in Rice et al. (2021) [21].

2.2. Experimental setup for plasma generation and preparation of PAW

Two types of cold plasma producing discharge setups, Spark and Glow, were used to generate the PAW described previously [22]. In both methods, a stainless-steel rod was used as the high-voltage electrode and fixed perpendicularly to a Petri dish containing 10 mL of deionised water. The distance between the water surface and the high-voltage electrode tip was fixed at 5 mm. To generate Spark discharge, the plastic Petri dish was placed on a stainless-steel plate which was connected to the ground (Fig. 1A); and to generate Glow discharge, a thin ground electrode rod was submerged into the water contained in the Petri dish (Fig. 1B); voltage was set to 4 kV for Spark and 2 kV for Glow, with an operating frequency of approximately 25 kHz, and treatment durations of 10, 20, and 30 min resulted in different PAW solutions designated here as Spark 10, Spark 20, and Spark 30, and Glow 10, Glow 20, and Glow 30. Both discharge setups were operated in open air.

2.3. Reactive Oxygen and Nitrogen Species (ROS/RNS) and pH quantification

The concentration of H_2O_2 in PAW was determined by mixing 10 μL titanium oxysulphate (IV) (Sigma Aldrich) solution with 100 μL of PAW, which produced yellow coloured pertitanic acid complex. Following a 10-min incubation period, absorbance was measured at 405 nm using a FLUOstar® Omega Multi-mode microplate reader (BMG Labtech, UK). The hydrogen peroxide concentration was then calculated from the standard curve.

The concentration of NO_3^- in PAW was determined photometrically by 2,6-dimethyl phenol (DMP) using the Nitrate Spectraquant Assay (Sigma Aldrich), as per the manufacturer's protocol. Both Spark and Glow PAW samples were pre-treated with sulfamic acid to eliminate the interference from NO_2^-. Following a 10-min incubation period in the dark at room temperature, absorbance was read at 540 nm using a FLUOstar® Omega Multi-mode microplate reader (BMG Labtech, UK). Nitrate concentration was calculated using the standard curve.

The Greiss test kit (Sigma Aldrich) was used to measure nitrite formation based on the colorimetric formation of N-alpha-napthyl-ethylenediamine from the reaction of nitrite and sulphanilamide. Samples were diluted by tenfold prior to testing, due to the long treatment time of the Glow discharge. 50 μL of sulphanilamide was added to either 50 μL of PAW or to 50 μL of nitrite standard and incubated for 5 min protected from light. Then, 50 μL of naphthyl-ethylenediamine was added to both the PAW samples and standards and incubated at room temperature protected from light for another 5 min.

The pH of the PAW solution was measured using a calibrated pH meter (Hanna, Edge), where sterile water was treated for 10, 20, and 30 min with either Spark or Glow discharge. The pH readings were taken immediately after generating the PAW, and readings were taken in triplicate.

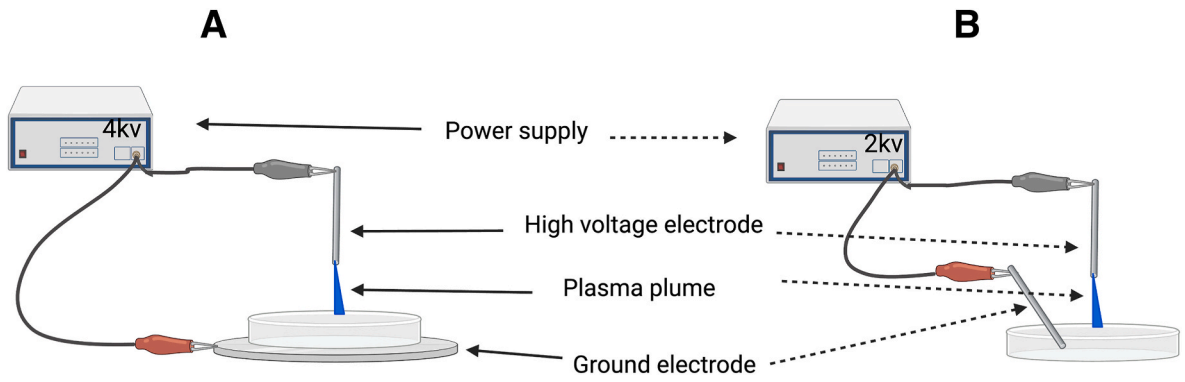

Fig. 1. Experimental setup for cold plasma generation. (A) Spark discharge setup with a 4 kV power supply connected to a high voltage electrode, producing a plasma plume directed at the target surface, and (B) Glow discharge configuration utilizing a 2 kV power supply with the high voltage electrode and associated plasma directed towards a liquid medium, both systems grounded through a secondary electrode. This schematic illustrates the differing electrical arrangements and plasma generation methods for experimental applications. Adapted from Lu et al., 2017 [22].

2.4. Susceptibility testing of planktonic and biofilm cultures

The susceptibility testing on planktonic cultures was carried out by initially adjusting the optical density (OD) of the overnight bacterial culture to an $OD_{600} = 0.1$, corresponding to 6×10^7 CFU/mL. Following this adjustment, 100 μL of the bacterial culture was combined with 900 μL of either Spark 10, Spark 20, Spark 30 or Glow 10, Glow 20, Glow 30 and mixed to ensure uniform interaction. At regular intervals of 10 min, ranging from 0 to 60 min, 20 μL samples were extracted from the mixture. Each of these samples underwent a tenfold serial dilution, after which they were cultured on low swarm agar plates to assess the bacterial susceptibility over time.

Next, we determined the susceptibility of PAW against biofilm cultures. Bacterial biofilms were cultivated on 1 cm long fragments of urinary catheter (Bard All-Silicone 14-Ch/Fr) for 24 h within a 24-well plate (Sigma Aldrich). The biofilms were then treated with either Spark 10, Spark 20, Spark 30 or Glow 10, Glow 20, Glow 30 for 60 min. At 10 min intervals, a catheter fragment was transferred to PBS, and then the bacterial cells were removed via sonication for 20 min. Following sonication, 20 μL of supernatant was serially diluted and plated on low swarm agar plate. These plates were incubated overnight at 37 °C, and the bacterial colonies were enumerated on the following day to determine the level of susceptibility exhibited by the biofilm cultures towards the PAW treatments.

2.5. Scavenger assay

Based on the susceptibility testing results, it was observed that Spark 30 and Glow 30 demonstrated the highest antibacterial activity. Consequently, further investigation into Spark 30 and Glow 30 was considered necessary. To identify the specific ROS/RNS contributing to antimicrobial activity of Spark 30 and Glow 30, various chemical scavengers were used, including sodium pyruvate (150 mM) for hydrogen peroxide [23], Tiron (20 mM) for superoxide ion [24], L-histidine (20 μm) for singlet oxygen and other ROS [25,26], haemoglobin (20 μm) for nitric oxide [27], and uric acid (100 μm) for ozone [28]. Along with bacterial culture, a respective scavenger was added to Spark 30 and Glow 30 PAW and the susceptibility testing was performed over 60 min, where every 10 min interval, 20 μL samples were aliquoted. These samples were serially diluted tenfold and plated on low swarm agar plates to determine the viable count.

2.6. Bacteriophage stability in PAW

The stability of the bacteriophage was assessed in Spark 30 and Glow 30 PAW. In brief, 100 μL of phage lysate (1×10^{11} PFU/mL) was mixed with 900 μL of either Spark 30 or Glow 30 PAW, followed by a 5 min incubation period at room temperature, with 10 μL aliquots of the treated phage lysate collected at 0, 1, 2-, 3-, 4-, and 5-min time points. The aliquoted samples were serially diluted in SM buffer, and a double-layered plaque assay was performed to determine the remaining viable phage particles after PAW treatment.

2.7. Combination treatment of PAW and phage against biofilm cells

The choice of the Spark 30 treatment method was informed by the results obtained from susceptibility testing on biofilms and stability study of ROS/RNS, with the objective of optimising our approach. Our study sought to assess the effectiveness of a combined strategy, which included the utilisation of Spark 30 PAW and phage treatment, in combatting *P. mirabilis* biofilms while determining the most efficacious treatment order for enhanced biofilm eradication. For viable cell counting, the bacterial biofilm was grown in LBB on a 1 cm long urinary catheter fragments (Bard All-Silicone 14-Ch/Fr) for 24 h in a 24-well plate in a static incubator at 37 °C.

Four treatment groups (phage only, PAW only, PAW followed by phage, phage followed by PAW) were compared with each other and no treatment control. The experimental design is presented in Fig. 2. In the phage only and phage followed by PAW groups, the biofilms grown on catheter fragments were exposed to phage PM-CJR solution (1.2×10^9 PFU/mL) for 24 h and then treated with Spark 30 PAW for 30 min in the phage followed by PAW group. In the PAW only and PAW followed by phage groups, the biofilms were treated with Spark 30 PAW first for 30 min and washed with PBS, after which the biofilms in the PAW followed by phage group were incubated in the PM-CJR solution (1.2×10^9 PFU/mL) for 24 h. Following individual and combinatorial treatments, biofilms from all four groups were washed with PBS prior to cell counting to remove planktonic bacteria. Biofilm cells were harvested by sonication in PBS for 20 min, serially diluted tenfold and plated on low swarm agar to enumerate viable cell counts.

2.8. Assessment of the biofilm biomass reduction following PAW and phage treatment

To determine the effect of Spark 30 PAW and phage treatment on biofilm biomass, we used the crystal violet (CV) assay. Biofilms were grown in LBB in a 96-well plate in the static incubator at 37 °C for 24 h and four treatment groups (phage only, PAW only, PAW followed by phage, phage followed by PAW) were compared with each other and no treatment control as described above (Fig. 2).

Following treatments, the media was discarded, and biofilms were washed with PBS to remove any planktonic cells. The biofilms were then allowed to dry for 15 min in a laminar flow hood. For staining, 0.1 % crystal violet solution was added to each well for 20 min, followed by a

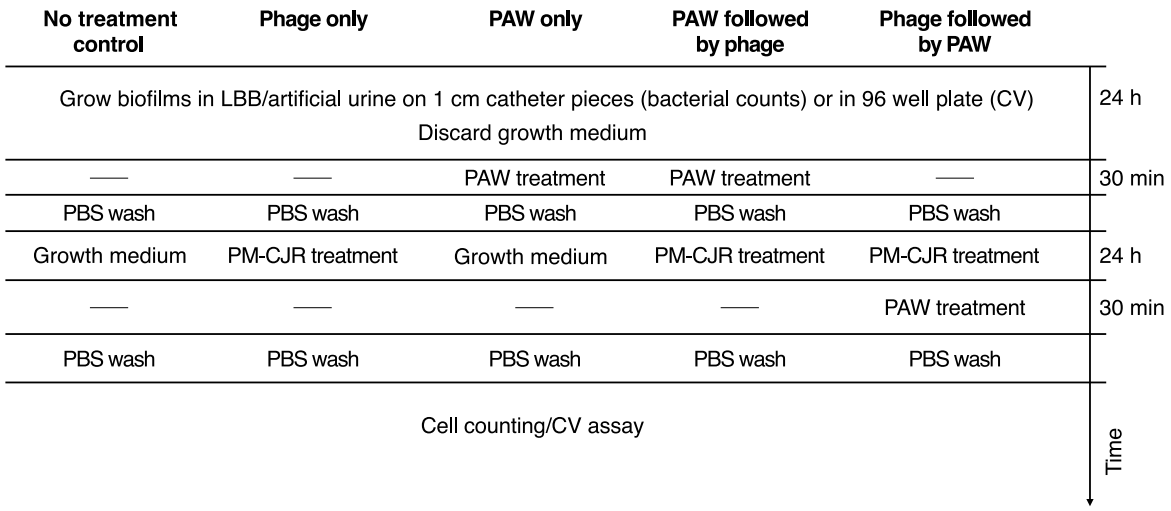

Fig. 2. Experimental design for the investigation of the effect of combinatorial treatments with PAW and phage on *P. mirabilis* biofilms. Phage PM-CJR was added in the same growth medium that was used to grow biofilms (either LBB or artificial urine).

thorough PBS rinse to remove excess stain. The plates were left in the laminar flow hood to dry overnight. The next day, 150 μL of 33 % acetic acid was added to each well to solubilise the bound crystal violet. After gentle mixing, 100 μL from each well was transferred to a new 96-well plate. The absorbance was then measured at 570 nm using a FLUOstar® Omega Multi-mode microplate reader (BMG Labtech, UK).

2.9. Combination treatment of spark 30 PAW and phage against biofilms formed in artificial urine

The PAW and phage combination treatment was tested against *Proteus mirabilis* BB2000 biofilm grown in artificial urine. Artificial urine was prepared by adapted Griffith model composition [29]. All chemicals were dissolved in 500 mL of deionised water and made up to a volume of 1000 mL (Table 1). The solution was left overnight on continuous stirring to ensure all components dissolved. The pH of the artificial urine was adjusted to 5.7 to 5.8 by adding 1 M HCl and NaOH and the solution was filtered through a 0.45 μm vacuum filter.

The biofilm was grown in artificial urine for 24 h on 1 cm long segments of the Bard All-Silicone 14-Ch/Fr urinary catheter for viable cell counting and in 96 well plates for the crystal violet assay. All experimental treatments, biofilm cell counting, and crystal violet staining were conducted as described above for the biofilms grown in LBB (Fig. 2), with four treatment groups (phage only, PAW only, phage followed by PAW, PAW followed by phage) compared to each other and to the bacterial growth control.

Table 1
Artificial urine composition.

Chemicals	Concentration (g/L)
Calcium chloride dehydrate	0.65
Magnesium chloride hexahydrate	0.65
Sodium chloride	4.60
Sodium sulfate	2.30
Trisodium citrate dehydrate	0.65
Sodium oxalate	0.02
Potassium dihydrogen phosphate	2.80
Potassium chloride	1.60
Ammonium chloride	1.00
Urea	25
Gelatine	1.10
Tryptone soya broth	1

2.10. Statistical analysis

One-way ANOVA with Dunnett's test was used for the analysis of results presented in Figs. 3–6. One-way ANOVA with Tukey's multiple comparison test against the untreated control (bacteria only) was used for Fig. 7. Statistically significant P values are represented by asterisks: * ($p < 0.05$), **($p < 0.01$), ***, ($p < 0.001$), and **** ($p < 0.0001$); ns – not significant. GraphPad Prism 10.0.3 was used for all analyses.

3. Results

Quantitative analysis of PAW treated with Spark and Glow discharge revealed differential generation of reactive species, as previously shown [22]. In Spark-treated PAW, the hydrogen peroxide concentration increased from 1.357 mM at 10 min to 1.984 mM at 30 min (Fig. 3A). No nitrite generation could be detected in Spark PAW (Fig. 3B), while the nitrate concentration levels increased from 139.04 mg/mL to 444.48 mg/mL (Fig. 3C). A trend of decreasing pH from 7.1 pH to final pH 1.67 was also observed with increasing Spark discharge duration (Fig. 3D). In Glow discharge-treated PAW, hydrogen peroxide was not detected at any time period, while nitrate concentrations increased from 228.26 mg/mL at 10 min to 452.15 mg/mL at 30 min (Fig. 3B) and nitrite levels increased from 223.80 μM to 348.15 μM (Fig. 3C), accompanied by a decline in pH from initial pH 7 to final pH 1.90 (Fig. 3D). It should be noted that while the most prominent changes happened within the first 10 min of treatment, statistically significant changes could be observed between 10 and 20 min treatment points as well as between 20 and 30 min treatment points, indicating that longer cold plasma treatment time leads to accumulation of additional ROS/RNS and results in more substantial pH decrease.

3.1. Bactericidal activity of PAW against Proteus mirabilis planktonic cells and biofilms

The bactericidal efficacy of PAW, treated with Spark and Glow discharges, was evaluated against *P. mirabilis* in both planktonic and biofilm states. In planktonic cultures treated with Spark discharge PAW (Fig. 4A), the water activated for 30 min (Spark 30) achieved complete bacterial eradication within 10 min, while the Spark 20 treatment resulted in 4-log reduction in bacterial count after 60 min. For Glow discharge treatments (Fig. 4B), Glow 30 demonstrated a robust 5-log reduction within 60 min, while the changes in cell numbers induced by Glow 20 and Glow 10 were below 3 log. When testing against

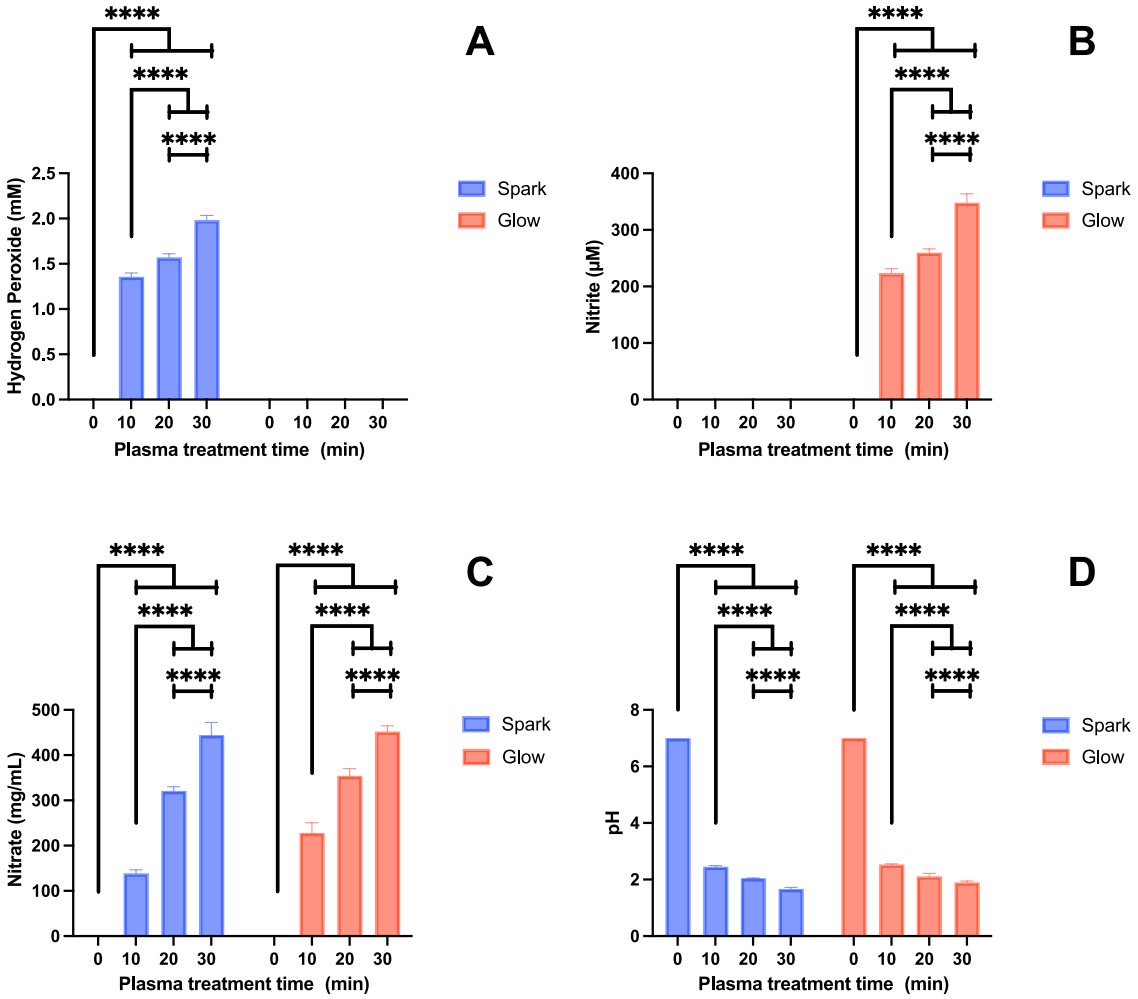

Fig. 3. Identification and quantification of ROS/RNS generated in deionised water following treatment exposure to Spark and Glow discharges, hydrogen peroxide (A), nitrite (B), nitrate (C), and pH (D). The error bars represent the mean ± standard deviation from three biological replicates. Asterisks indicate significant differences between the relevant exposure times compared to baseline (time = 0), * ($p < 0.05$), **($p < 0.01$), ***, ($p < 0.001$), and **** ($p < 0.0001$) using one-way ANOVA and Dunnett's post-test analysis (n = 3).

biofilms, neither Spark nor Glow discharge PAW achieved the same level of efficacy as observed with planktonic cells. Spark discharge PAW (Fig. 4C) at the 30-min exposure (Spark 30) resulted in a 1.5-log reduction within 60 min. The shorter exposure times, Spark 20 and Spark 10, each led to reductions lower than 1 log. Glow discharge PAW (Fig. 4D) displayed a similar trend with Glow 30 showing the greatest decrease in log CFU/mL. Based on the results of this experiment, Spark 30 and Glow 30 were used in all subsequent tests given their more prominent antimicrobial properties.

3.2. Scavenger assay

The scavenger assay was used to identify what reactive species present in PAW contribute to its antimicrobial activity against *P. mirabilis*. In the presence of Spark 30 PAW (Fig. 5A), the addition of sodium pyruvate, a hydrogen peroxide scavenger, resulted in significant survival rates of 7 log CFU/mL after 60 min. This suggests a key role for hydrogen peroxide in the bactericidal activity of Spark 30 PAW. Similarly, L-histidine addition led to a comparable survival count. In contrast, scavengers like uric acid, Tiron, and haemoglobin did not impair the bactericidal action of Spark 30 PAW, indicating that ozone, superoxide anions, and nitric oxide may not play a major role in the observed bactericidal activity.

For Glow 30 PAW (Fig. 5B), only the introduction of L-histidine significantly reduced bactericidal efficacy, leaving 7 log CFU/mL surviving bacteria after 60 min of treatment with Glow 30 PAW treated with L-histidine. Conversely, when other scavengers such as sodium pyruvate, uric acid, Tiron, and haemoglobin were added to Glow 30 PAW, they did not impede its bactericidal activity, as bacterial counts dropped to around 2 log CFU/mL after 60 min of treatment with Glow 30 supplemented with ROS/RNS scavengers.

3.3. Bacteriophage stability in PAW

The assessment of phage susceptibility to PAW was conducted using Spark 30 and Glow 30 PAW, as illustrated in Fig. 6. The findings reveal the differences in stability of phage PM-CJR in PAW generated to Spark and Glow discharge treatments. Specifically, in Spark 30 discharge PAW, a 5-log reduction in phage titre was detected within a 5-min interval. In contrast, Glow 30 discharge PAW exhibited a faster inactivation of phage, achieving complete inactivation within only 4 min. These results illustrate the differential impacts of Spark and Glow discharge treatments on the stability and viability of phage PM-CJR in PAW.

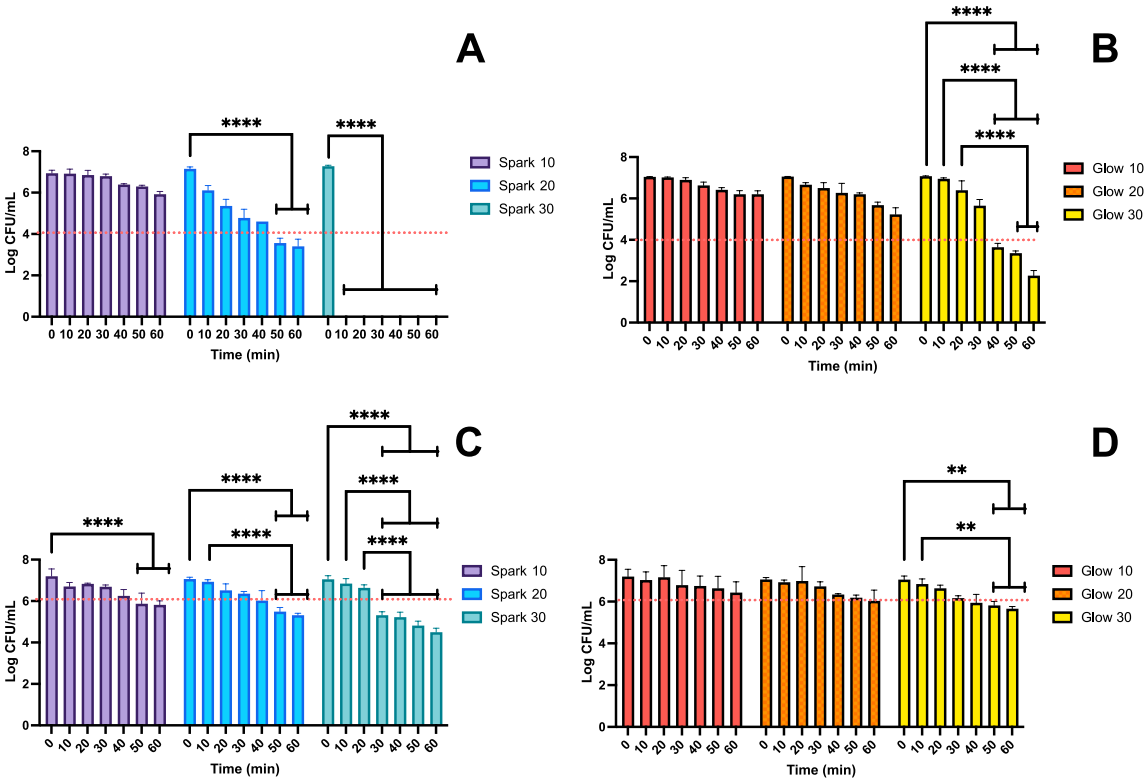

Fig. 4. Bactericidal effects of Spark and Glow discharge generated PAW against *P. mirabilis* in planktonic (A, B) and biofilm (C, D) states. The error bars represented the mean ± standard deviation from three biological replicates. Asterisks indicate significant differences between the relevant exposure times, * ($p < 0.05$), **($p < 0.01$), ***, ($p < 0.001$), and **** ($p < 0.0001$) using one-way ANOVA and Dunnett's post-test analysis (n = 3).

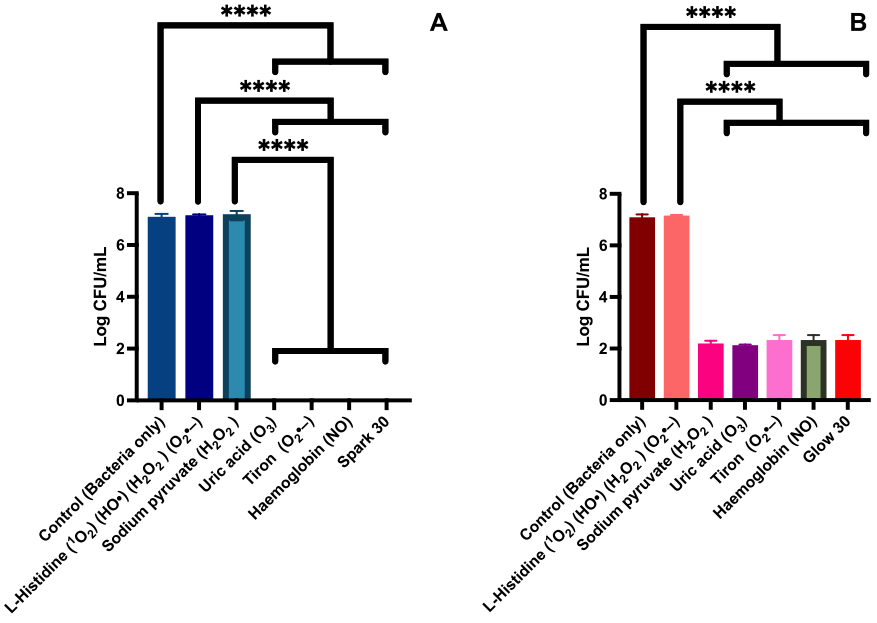

Fig. 5. Impact of chemical scavengers on the antimicrobial activity of Spark 30 (A) and Glow 30 (B) PAW treatments against *P. mirabilis*. The bars represent the mean bacterial count following treatment with scavengers targeting hydrogen peroxide (sodium pyruvate), singlet oxygen and other longer-living ROS (L-histidine), ozone (uric acid), superoxide anions (O_2^-) (Tiron), and nitric oxide (haemoglobin). The error bars represent the mean ± standard deviation from three biological replicates, asterisks indicate significant differences between the control (bacteria only) and treated groups, * ($p < 0.05$), **($p < 0.01$), ***, ($p < 0.001$), and **** ($p < 0.0001$) using one-way ANOVA and Dunnett's post-test analysis (n = 3).

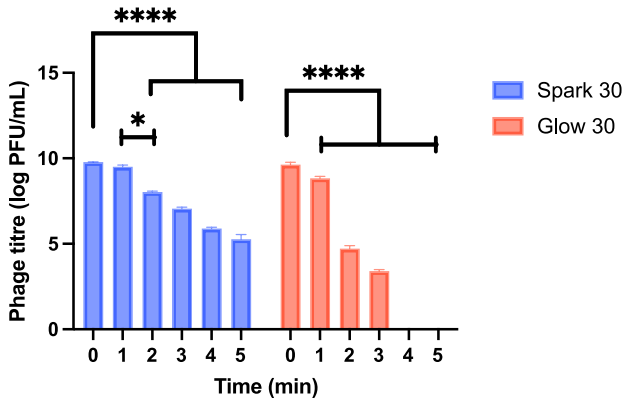

Fig. 6. Stability of phage PM-CJR in Spark 30 (●) and Glow 30 (■) discharge treated PAW. The error bars represent the mean ± standard deviation from three biological replicates, asterisks indicate significant differences between the relevant exposure times compared to baseline (time = 0), * ($p < 0.05$), **($p < 0.01$), ***, ($p < 0.001$), and **** ($p < 0.0001$) using one-way ANOVA and Dunnett's post-test analysis (n = 3).

3.4. Combination treatment efficacy against Proteus mirabilis biofilm

The efficacy of combined PAW and phage treatments against *P. mirabilis* biofilm grown in LBB was assessed (Fig. 7A). Spark 30 PAW was chosen for this experiment due to its more pronounced bactericidal effect and higher phage stability in Spark 30 compared to Glow 30. Treatment with Spark 30 PAW, followed by the application of a 1.2×10^9 PFU/mL phage solution for 24 h, significantly reduced the bacterial load in the biofilm by more than 4-log. In comparison, reversing this sequence to phage followed by Spark 30 resulted in ~1.5 log reduction. The individual treatments with PAW or phage alone achieved similar ~1.5 log reductions, demonstrating the enhanced efficacy of the sequential combination treatment when Spark 30 PAW is used first.

The crystal violet assay, correlating absorbance with biofilm biomass, showed all treatments significantly reduced biofilm compared to the untreated control (Fig. 7B). The control group showed an absorbance of 0.47, whereas the Spark 30 PAW and phage treatments alone resulted in absorbances of 0.07 and 0.18, respectively. The combined treatment with Spark 30 PAW followed by phage yielded the lowest absorbance of 0.01, indicating the most substantial reduction in biofilm biomass.

The results of the experiments on biofilms grown in artificial urine instead of LBB demonstrated a similar pattern. The combination treatment with Spark 30 PAW and phage showed a 4 log reduction in bacterial population after 24 h (Fig. 7C), whereas the individual treatment of PAW and phage showed around 2 log reduction, similar to the combinatorial treatment with phage followed by PAW treatment. The individual treatments with phage and Spark 30 PAW showed no statistically significant difference when compared to each other. The biomass of the biofilm grown in artificial urine was determined by the crystal violet assay method after the subsequent treatment with Spark 30 PAW and phage (Fig. 7D). The crystal violet assay for the bacteria only control group showed 0.5 absorbance at 570 nm, while phage only and Spark 30 only individual treatments showed 0.12 and 0.22 absorbance respectively. On the other hand, the combination treatment of Spark 30 followed by phage resulted in approximately 0.05 absorbance units, thus outperforming both the individual treatments and phage followed by Spark 30 PAW combinatorial treatment in terms of biofilm dispersion.

4. Discussion

This study provides initial insights into the possibility of combining PAW and phage treatment against *P. mirabilis* biofilm. PAW produced with Spark and Glow discharge exhibits potent antibacterial activity against planktonic and biofilm phenotypes of *P. mirabilis*. These results correlate with previous findings which demonstrated the antibacterial properties of PAW against various Gram-positive and Gram-negative pathogens [22,30–33].

The bactericidal impact of both Spark PAW and Glow PAW is proportional to the duration of exposure of water to the cold plasma discharge. While Glow 30 had lower activity compared to Spark 30 PAW at 60 min, the treatment of *P. mirabilis* with Glow 30 had non-linear kill dynamics with a noticeable decrease in the viable cell counts between 30 and 40 min of treatment. Spark PAW exhibited more potent activity compared to Glow PAW at each exposure time. Biofilms have demonstrated increased resilience against PAW treatments relative to planktonic forms, aligning with past research [34,35]. Prior studies demonstrated that extracellular polymeric substances (EPS) in biofilms mediate tolerance to plasma treatments, potentially through the sequestration of reactive species by biofilm components [36]. This interaction between the reactive species and the biofilm matrix may underlie the observed lower bactericidal activity of PAW against biofilms.

In investigating the antimicrobial mechanisms of Spark 30 and Glow 30 PAW, the scavenger assays allowed to gain insights into the roles of several potential ROS/RNS. While we have quantified some of the longer-lived reactive species, measurement of short-lived ROS/RNS is problematic, making accurate characterisation of the full profile of reactive species in PAW difficult [37]. The scavenger assays indicate that hydrogen peroxide (sodium pyruvate) and various unidentified ROS (L-histidine) are major contributors to antibacterial activity in PAW. Hydrogen peroxide is a potent oxidising agent that damages bacterial cells through multiple mechanisms, such as oxidative stress against biofilm [11]. Similar effects were observed when L-histidine was added to Spark 30 and Glow 30 PAW, resulting in complete survival of *P. mirabilis*. While L-histidine is often used a singlet oxygen scavenger, it can also efficiently scavenge other ROS, including H_2O_2. This indicates that while the precise ROS responsible for the observed antimicrobial effects in PAW are challenging to pinpoint due to their transient nature, the influence of other stable ROS or their derivatives inactivated by these scavengers, particularly in the case of Spark PAW, cannot be disregarded. It is therefore suggested that a combination of different ROS may play a key role in the bactericidal activity of PAW. Several studies have previously explored the effects of PAW on pathogenic bacteria [38–40]. Of note, Tsoukou et al. employed the same plasma generation system used in this study and revealed that Glow discharge PAW was either as effective or exhibited superior efficacy to Spark discharge in eradicating planktonic *Escherichia coli* and *Staphylococcus aureus* [40]. In a more recent study, the antibacterial activity of four plasma-activated liquid preparations was assessed against a pathogenic *E. coli* strain, with higher efficacy of Glow discharge relative to other generation methodologies also being reported [41]. However, a different cold plasma generation device was used, and various factors could contribute to these disparities, such as voltage or positioning of the ground electrode, thus impacting the pH as well as concentrations and ratios of different ROS/RNS within a PAW. Indeed, while in our study both types of discharge resulted in a rapid decrease of pH and accumulation of nitrate ions in PAW, hydrogen peroxide was detected only in Spark PAW, while nitrite formation occurred only in Glow PAW.

Next, we focused on investigating the antibiofilm effects of combinations of PAW and phage solutions. Given the potent antimicrobial effect of PAW, we first tested phage stability in PAW. The observation that bacteriophages were also susceptible to both Spark and Glow PAW was similar to previous studies which demonstrated that direct treatment of cold plasma and PAW deactivated the viable phage particles by damaging phage genomic nucleic acid and phage capsid proteins [42,43]. Complete inactivation of phage in Glow 30 PAW was achieved within 4 min. Interestingly, the rate of phage decay in Spark 30 was

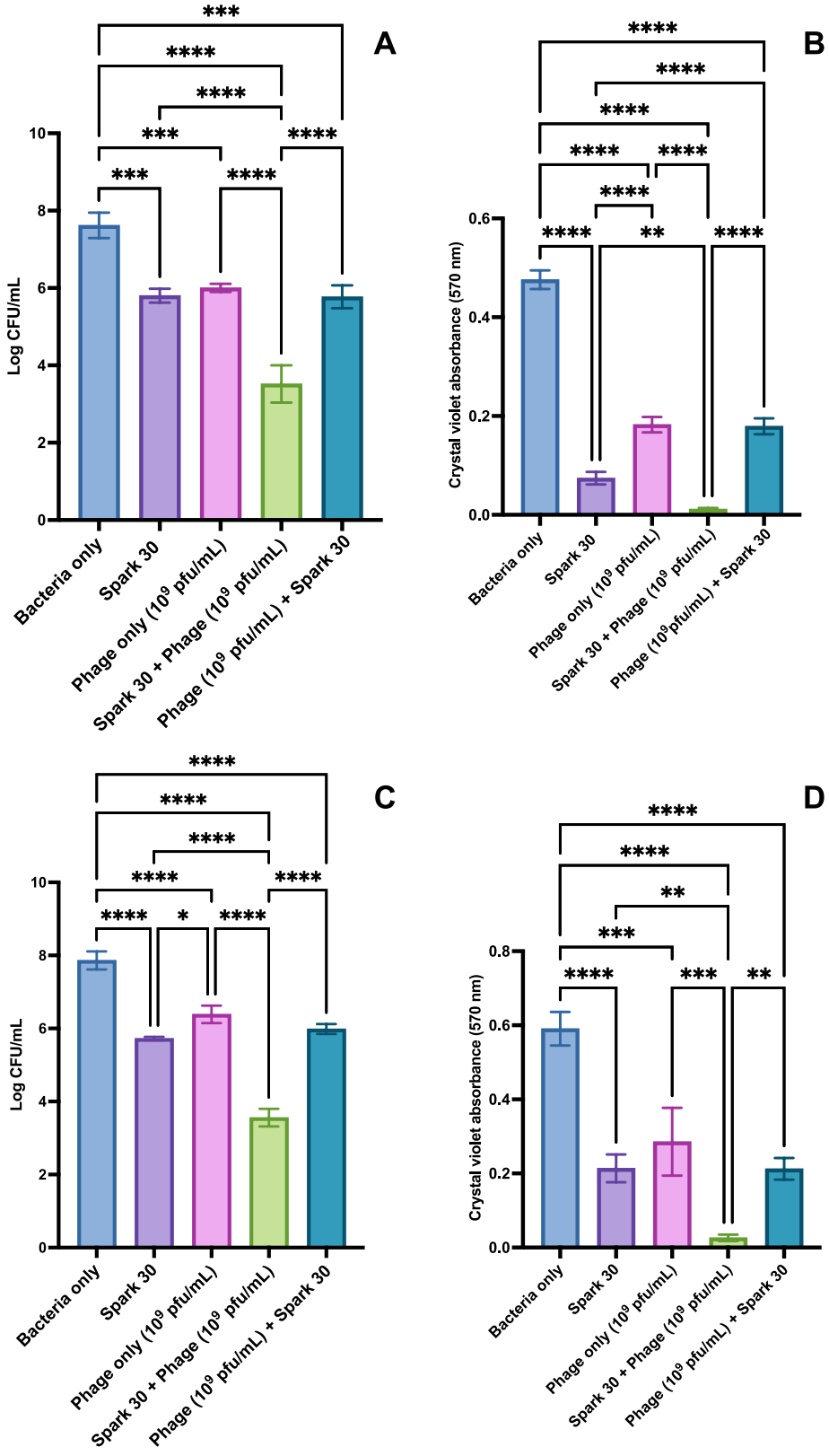

Fig. 7. The combination treatment results of Spark 30 PAW and phage against the biofilm formed in LBB (top panels) and artificial urine (bottom panels). (A, C) Bacterial titre reduction. (B, D) Biofilm biomass reduction measured by crystal violet assay. PAW followed by phage treatment exhibited superior efficacy of reduction of bacterial cells within the biofilm than both the individual and phage followed by PAW treatment. Similarly, biofilm biomass decrease was most notable in the PAW followed by phage treatment group. The error bars represent the mean ± standard deviation from three biological replicates, asterisks indicate significant differences between the untreated (bacteria only) and treated groups * ($p < 0.05$), **($p < 0.01$), ***, ($p < 0.001$), and **** ($p < 0.0001$) using one-way ANOVA and Tukey's post-test analysis ($n = 3$). (For interpretation of the references to colour in this figure legend, the reader is referred to the Web version of this article.)

lower compared to Glow 30. This inactivating effect of PAW on phages suggested that a direct co-administration of a mixture of PAW and phages would be ineffective.

Following the antimicrobial assays against both planktonic and biofilm models, Spark 30 was identified as the most effective PAW. Given the susceptibility of phages to PAW, sequential administration of PAW and phages was tested, both in LBB and in artificial urine (Fig. 7). A substantial reduction in bacterial load was observed with Spark 30 PAW followed by phage treatment resulting in at least 4-log reduction of cell counts in biofilms grown in either medium; interestingly, there was no difference between the combinatorial and phage-only treatments when the reverse order of treatment (phage followed by Spark PAW 30) was tested. The potentiating effect of hydrogen peroxide (present in Spark PAW 30) and other ROS on the bactericidal activity of phages has previously been reported [44,45]. Bacterial cell filamentation caused by ROS is often mentioned to be one of the key mechanisms responsible for this. However, the pre-treatment with PAW might also alter the physical and chemical properties of the biofilm, thereby enhancing the penetration and bactericidal activity of the phage or lead to biofilm matrix dispersal. The crystal violet assay provided further evidence of this interaction, revealing a dramatic reduction in biofilm biomass. Specifically, treatment with PAW followed by phage therapy led to an estimated 97 % decrease in biomass, while reversing the order of treatment yielded only a 60 % reduction. When applied individually, treatments with PAW and phage resulted in 70 % and 55 % reductions, respectively. The antibiofilm activity of PAW thus appears to be significantly amplified by the introduction of phage PM-CJR. This phage's depolymerase activity specifically targets the biofilm matrix by degrading extracellular polysaccharides [21,46], which might contribute to the pronounced biofilm-disrupting effect of the Spark 30 PAW-phage combination.

While cold plasma systems and applications are being actively developed and used for the purposes of disinfection and decontamination in the agri-food sector, plasma medicine is an emerging field, and most studies reported to date were conducted in vitro or using animal models. In addition, the necessity of a direct exposure of a treated surface to the plasma discharge limits its potential biomedical applications; plasma activated liquids present an alternative approach that can be used in situations when a plasma discharge cannot reach its target. Of special interest in the context of the present investigation is thus a study by Pastorek et al. (2022), in which the authors demonstrated in vitro antibacterial effectiveness of a specific plasma-activated liquid against an uropathogenic strain of *E. coli* [41]. However, its application in a murine UTI model did not result in improved outcomes, possibly due to interactions between the plasma activated liquid, urinary constituents, and the host's immune response.

Several studies have demonstrated that cold plasma and PAW can be used for pre-treatment, potentiating the anti-biofilm activity of routinely used topical antibiotics and antiseptics [11]. Although phage therapy has been successfully applied to treatment of urinary tract infections [47–49], CAUTIs present additional challenges. Biofilm matrices confer physical protection to bacteria encased in them, while the physiology of bacteria inside biofilms differs significantly from that of planktonic cells, impeding bacterial killing by phages. However, Cui et al. (2018) demonstrated that by combining treatments with cold nitrogen plasma and phage, a significant 5-log reduction of *E. coli* biofilms could be achieved [16]. Finally, Evran et al. recently published a study on the sequential treatment with PAW and phage of *Salmonella enterica* serovar Typhimurium on lettuce leaves. Interestingly, in their study phage application followed by PAW treatment was more efficient compared to the reverse order, which was more efficient in our experiments [50]. Whilst our study focused on the combination of PAW and phage against a human pathogen *P. mirabilis* grown as biofilms on silicone catheters, the work of Evran et al. further confirms the importance of order of application of PAW and phage in enhancing their antimicrobial activities.

The escalating issue of AMR underscores the urgency for alternative therapeutic strategies, especially given the challenges posed by biofilm-forming uropathogens in CAUTIs. This study demonstrates that Spark and Glow discharge PAW are effective against *P. mirabilis* biofilms, with Spark showing a more prominent antibacterial effect. The sequential application of Spark 30 PAW followed by phage further significantly reduced biofilm biomass and bacterial load; the reverse order (phage followed by PAW) did not show better antibacterial effects compared to using Spark PAW or phage alone. We hypothesise that PAW can disrupt biofilm structures, thus enhancing phage penetration and bactericidal action, but further investigations will be required to elucidate the physical and chemical processes responsible for this effect. Nevertheless, our study demonstrates the feasibility of using combinations of plasma-activated water and phage against biofilm-associated infections and highlights their potential as the basis of future therapeutic interventions, including for the management of UTIs.

CRediT authorship contribution statement

Akash Shambharkar: Writing – review & editing, Writing – original draft, Visualization, Validation, Methodology, Investigation, Formal analysis, Data curation, Conceptualization. **Thomas P. Thompson:** Writing – review & editing, Writing – original draft, Methodology, Investigation, Conceptualization. **Laura A. McClenaghan:** Writing – review & editing, Writing – original draft, Methodology, Investigation, Formal analysis, Data curation, Conceptualization. **Paula Bourke:** Writing – review & editing, Resources. **Brendan F. Gilmore:** Writing – review & editing, Resources. **Timofey Skvortsov:** Writing – review & editing, Supervision, Resources, Project administration, Funding acquisition, Conceptualization.

Declaration of competing interest

The authors declare the following financial interests/personal relationships which may be considered as potential competing interests: Akash Shambharkar reports financial support was provided by Maharashtra State Board of Technical Education. If there are other authors, they declare that they have no known competing financial interests or personal relationships that could have appeared to influence the work reported in this paper.

Data availability

All data generated or analysed during this study are included.

References

[1] Guest JF, Keating T, Gould D, Wigglesworth N. Modelling the annual NHS costs and outcomes attributable to healthcare-associated infections in England. BMJ Open 2020;10:e033367. https://doi.org/10.1136/bmjopen-2019-033367.
[2] Loveday HP, Wilson JA, Pratt RJ, Golsorkhi M, Tingle A, Bak A, et al. epic 3: national evidence-based guidelines for preventing healthcare-associated infections in NHS hospitals in England. J Hosp Infect 2014;86:S1–70. https://doi.org/10.1016/S0195-6701(13)60012-2.
[3] Nicolle LE. Catheter associated urinary tract infections. Antimicrob Resist Infect Control 2014;3:23. https://doi.org/10.1186/2047-2994-3-23.
[4] Letica-Kriegel AS, Salmasian H, Vawdrey DK, Youngerman BE, Green RA, Furuya EY, et al. Identifying the risk factors for catheter-associated urinary tract infections: a large cross-sectional study of six hospitals. BMJ Open 2019;9: e022137. https://doi.org/10.1136/bmjopen-2018-022137.
[5] Wasfi R, Hamed SM, Amer MA, Fahmy LI. Proteus mirabilis biofilm: development and therapeutic strategies. Front Cell Infect Microbiol 2020;10. https://doi.org/10.3389/fcimb.2020.00414.
[6] Yuan F, Huang Z, Yang T, Wang G, Li P, Yang B, et al. Pathogenesis of Proteus mirabilis in catheter-associated urinary tract infections. Urol Int 2021;105:354–61. https://doi.org/10.1159/000514097.
[7] Pelling H, Nzakizwanayo J, Milo S, Denham EL, MacFarlane WM, Bock LJ, et al. Bacterial biofilm formation on indwelling urethral catheters. Lett Appl Microbiol 2019;68:277–93. https://doi.org/10.1111/lam.13144.
[8] Murray CJL, Ikuta KS, Sharara F, Swetschinski L, Aguilar GR, Gray A, et al. Global burden of bacterial antimicrobial resistance in 2019: a systematic analysis. Lancet 2022;399:629–55. https://doi.org/10.1016/S0140-6736(21)02724-0.

[9] Gilmore BF, Flynn PB, O'Brien S, Hickok N, Freeman T, Bourke P. Cold plasmas for biofilm control: opportunities and challenges. Trends Biotechnol 2018;36:627–38. https://doi.org/10.1016/j.tibtech.2018.03.007.

[10] Flynn PB, Higginbotham S, Alshraiedeh NH, Gorman SP, Graham WG, Gilmore BF. Bactericidal efficacy of atmospheric pressure non-thermal plasma (APNTP) against the ESKAPE pathogens. Int J Antimicrob Agents 2015;46:101–7. https://doi.org/10.1016/j.ijantimicag.2015.02.026.

[11] Maybin J-A, Thompson TP, Flynn PB, Skvortsov T, Hickok NJ, Freeman TA, et al. Cold atmospheric pressure plasma-antibiotic synergy in *Pseudomonas aeruginosa* biofilms is mediated via oxidative stress response. Biofilm 2023;5:100122. https://doi.org/10.1016/j.bioflm.2023.100122.

[12] Melo LDR, Veiga P, Cerca N, Kropinski AM, Almeida C, Azeredo J, et al. Development of a phage cocktail to control Proteus mirabilis catheter-associated urinary tract infections. Front Microbiol 2016;7. https://doi.org/10.3389/fmicb.2016.01024.

[13] Sanchez BC, Heckmann ER, Green SI, Clark JR, Kaplan HB, Ramig RF, et al. Development of phage cocktails to treat E. coli catheter-associated urinary tract infection and associated biofilms. Front Microbiol 2022;13. https://doi.org/10.3389/fmicb.2022.796132.

[14] Łusiak-Szelachowska M, Międzybrodzki R, Drulis-Kawa Z, Cater K, Knežević P, Winogradow C, et al. Bacteriophages and antibiotic interactions in clinical practice: what we have learned so far. J Biomed Sci 2022;29:23. https://doi.org/10.1186/s12929-022-00806-1.

[15] Townsend EM, Moat J, Jameson E. CAUTI's next top model – model dependent *Klebsiella* biofilm inhibition by bacteriophages and antimicrobials. Biofilm 2020;2:100038. https://doi.org/10.1016/j.bioflm.2020.100038.

[16] Cui H, Bai M, Yuan L, Surendhiran D, Lin L. Sequential effect of phages and cold nitrogen plasma against *Escherichia coli* O157:H7 biofilms on different vegetables. Int J Food Microbiol 2018;268:1–9. https://doi.org/10.1016/j.ijfoodmicro.2018.01.004.

[17] Gu X, Huang D, Chen J, Li X, Zhou Y, Huang M, et al. Bacterial inactivation and biofilm disruption through indigenous prophage activation using low-intensity cold atmospheric plasma. Environ Sci Technol 2022;56:8920–31. https://doi.org/10.1021/acs.est.2c01516.

[18] Braný D, Dvorská D, Halašová E, Škovierová H. Cold atmospheric plasma: a powerful tool for modern medicine. Int J Mol Sci 2020;21:2932. https://doi.org/10.3390/ijms21082932.

[19] Murillo D, Huergo C, Gallego B, Rodríguez R, Tornín J. Exploring the use of cold atmospheric plasma to overcome drug resistance in cancer. Biomedicines 2023;11:208. https://doi.org/10.3390/biomedicines11010208.

[20] Sullivan NL, Septer AN, Fields AT, Wenren LM, Gibbs KA. The complete genome sequence of Proteus mirabilis strain BB2000 reveals differences from the P. mirabilis reference strain. Genome Announc 2013;1:e00024. https://doi.org/10.1128/genomeA.00024-13. 13.

[21] Rice CJ, Kelly SA, O'Brien SC, Melaugh EM, Ganacias JCB, Chai ZH, et al. Novel phage-derived depolymerase with activity against Proteus mirabilis biofilms. Microorganisms 2021;9:2172. https://doi.org/10.3390/microorganisms9102172.

[22] Lu P, Boehm D, Bourke P, Cullen PJ. Achieving reactive species specificity within plasma-activated water through selective generation using air spark and glow discharges. Plasma Process Polym 2017;14:1600207. https://doi.org/10.1002/ppap.201600207.

[23] Kelts JL, Cali JJ, Duellman SJ, Shultz J. Altered cytotoxicity of ROS-inducing compounds by sodium pyruvate in cell culture medium depends on the location of ROS generation. SpringerPlus 2015;4:269. https://doi.org/10.1186/s40064-015-1063-y.

[24] Guo L, Yao Z, Yang L, Zhang H, Qi Y, Gou L, et al. Plasma-activated water: an alternative disinfectant for S protein inactivation to prevent SARS-CoV-2 infection. Chem Eng J 2021;421:127742. https://doi.org/10.1016/j.cej.2020.127742.

[25] Dogra V, Kim C. Singlet oxygen metabolism: from genesis to signaling. Front Plant Sci 2020;10. https://doi.org/10.3389/fpls.2019.01640.

[26] Xiao A, Liu D, Li Y. Plasma-activated tap water production and its application in atomization disinfection. Appl Sci 2023;13:3015. https://doi.org/10.3390/app13053015.

[27] Rothwell JG, Alam D, Carter DA, Soltani B, McConchie R, Zhou R, et al. The antimicrobial efficacy of plasma-activated water against Listeria and E. coli is modulated by reactor design and water composition. J Appl Microbiol 2022;132:2490–500. https://doi.org/10.1111/jam.15429.

[28] Zhang C, Brown PJB, Miles RJ, White TA, Grant DG, Stalla D, et al. Inhibition of regrowth of planktonic and biofilm bacteria after peracetic acid disinfection. Water Res 2019;149:640–9. https://doi.org/10.1016/j.watres.2018.10.062.

[29] Moore JV, Kim D, Irwin NJ, Rimer JD, McCoy CP. Tetrasodium EDTA for the prevention of urinary catheter infections and blockages. RSC Adv 2023;13:2202–12. https://doi.org/10.1039/D2RA06418A.

[30] Hadinoto K, Astorga JB, Masood H, Zhou R, Alam D, Cullen PJ, et al. Efficacy optimization of plasma-activated water for food sanitization through two reactor design configurations. Innovat Food Sci Emerg Technol 2021;74:102867. https://doi.org/10.1016/j.ifset.2021.102867.

[31] Liu X, Li Y, Wang S, Huangfu L, Zhang M, Xiang Q. Synergistic antimicrobial activity of plasma-activated water and propylparaben: mechanism and applications for fresh produce sanitation. LWT 2021;146:111447. https://doi.org/10.1016/j.lwt.2021.111447.

[32] Małajowicz J, Khachatryan K, Kozłowska M. Properties of water activated with low-temperature plasma in the context of microbial activity. Beverages 2022;8:63. https://doi.org/10.3390/beverages8040063.

[33] Mentheour R, Machala Z. Coupled antibacterial effects of plasma-activated water and pulsed electric field. Front Physiol 2022;10. https://doi.org/10.3389/fphy.2022.895813.

[34] Basiri N, Zarei M, Kargar M, Kafilzadeh F. Effect of plasma-activated water on the biofilm-forming ability of *Salmonella enterica* serovar Enteritidis and expression of the related genes. Int J Food Microbiol 2023;406:110419. https://doi.org/10.1016/j.ijfoodmicro.2023.110419.

[35] Smet C, Govaert M, Kyrylenko A, Easdani M, Walsh JL, Van Impe JF. Inactivation of single strains of Listeria monocytogenes and Salmonella Typhimurium planktonic cells biofilms with plasma activated liquids. Front Microbiol 2019;10. https://doi.org/10.3389/fmicb.2019.01539.

[36] Alshraiedeh NH, Kelly SA, Thompson TP, Flynn PB, Tunney MM, Gilmore BF. Extracellular polymeric substance-mediated tolerance of Pseudomonas aeruginosa biofilms to atmospheric pressure nonthermal plasma treatment. Plasma Process Polym 2020;17:2000108. https://doi.org/10.1002/ppap.202000108.

[37] Wu M-C, Uehara S, Wu J-S, Xiao Y, Nakajima T, Sato T. Dissolution enhancement of reactive chemical species by plasma-activated microbubbles jet in water. J Phys D Appl Phys 2020;53:485201. https://doi.org/10.1088/1361-6463/abae96.

[38] Chen T-P, Liang J, Su T-L. Plasma-activated water: antibacterial activity and artifacts? Environ Sci Pollut Res 2018;25:26699–706. https://doi.org/10.1007/s11356-017-9169-0.

[39] Li Y, Pan J, Ye G, Zhang Q, Wang J, Zhang J, et al. In vitro studies of the antimicrobial effect of non-thermal plasma-activated water as a novel mouthwash. Eur J Oral Sci 2017;125:463–70. https://doi.org/10.1111/eos.12374.

[40] Tsoukou E, Delit M, Treint L, Bourke P, Boehm D. Distinct chemistries define the diverse biological effects of plasma activated water generated with spark and glow plasma discharges. Appl Sci 2021;11:1178. https://doi.org/10.3390/app11031178.

[41] Pastorek M, Suchoňová M, Konečná B, Pásztor S, Petrus J, Ivašková N, et al. The effect of air plasma activated liquid on uropathogenic bacteria. Plasma Chem Plasma Process 2022;42:561–74. https://doi.org/10.1007/s11090-022-10239-1.

[42] Guo L, Xu R, Gou L, Liu Z, Zhao Y, Liu D, et al. Mechanism of virus inactivation by cold atmospheric-pressure plasma and plasma-activated water. Appl Environ Microbiol 2018;84:e00726. https://doi.org/10.1128/AEM.00726-18. 18.

[43] Upadrasta A, Daniels S, Thompson TP, Gilmore B, Humphreys H. In situ generation of cold atmospheric plasma-activated mist and its biocidal activity against surrogate viruses for COVID-19. J Appl Microbiol 2023;134:lxad181. https://doi.org/10.1093/jambio/lxad181.

[44] Kim M, Jo Y, Hwang YJ, Hong HW, Hong SS, Park K, et al. Phage-antibiotic synergy via delayed lysis. Appl Environ Microbiol 2018;84:e02085. https://doi.org/10.1128/AEM.02085-18. 18.

[45] Li X, Hu T, Wei J, He Y, Abdalla AE, Wang G, et al. Characterization of a novel bacteriophage Henu2 and evaluation of the synergistic antibacterial activity of phage. Antibiotics 2021;10. https://doi.org/10.3390/antibiotics10020174.

[46] Chang C, Yu X, Guo W, Guo C, Guo X, Li Q, et al. Bacteriophage-Mediated control of biofilm: a promising new dawn for the future. Front Microbiol 2022;13. https://doi.org/10.3389/fmicb.2022.825828.

[47] Al-Anany AM, Hooey PB, Cook JD, Burrows LL, Martyniuk J, Hynes AP, et al. Phage therapy in the management of urinary tract infections: a comprehensive systematic review. PHAGE 2023;4:112–27. https://doi.org/10.1089/phage.2023.0024.

[48] Leitner L, Ujmajuridze A, Chanishvili N, Goderdzishvili M, Chkonia I, Rigvava S, et al. Intravesical bacteriophages for treating urinary tract infections in patients undergoing transurethral resection of the prostate: a randomised, placebo-controlled, double-blind clinical trial. Lancet Infect Dis 2021;21:427–36. https://doi.org/10.1016/S1473-3099(20)30330-3.

[49] Zulk JJ, Patras KA, Maresso AW. The rise, fall, and resurgence of phage therapy for urinary tract infection. EcoSal Plus 2024. https://doi.org/10.1128/ecosalplus.esp-0029-2023. 0:eesp-0029-2023.

[50] Evran E, Dasan BG, Tayyarcan EK, Boyaci IH. Effect of sequential treatment of plasma activated water and bacteriophage on decontamination of Salmonella Typhimurium in lettuce. Food Bioprocess Technol 2024. https://doi.org/10.1007/s11947-024-03355-7.